

# From reaching to reach-to-grasp: the arm posture difference and its implications on human motion control strategy

Zhi Li<sup>1</sup>  · Dejan Milutinović<sup>2</sup> · Jacob Rosen<sup>3</sup>

Received: 12 May 2016 / Accepted: 23 January 2017 / Published online: 6 March 2017  
© Springer-Verlag Berlin Heidelberg 2017

**Abstract** Reach-to-grasp arm postures differ from those in pure reaching because they are affected by grasp position/orientation, rather than simple transport to a position during a reaching motion. This paper investigates this difference via an analysis of experimental data collected on reaching and reach-to-grasp motions. A seven-degree-of-freedom (DOFs) kinematic arm model with the swivel angle is used for the motion analysis. Compared to a widely used anatomical arm model, this model distinguishes clearly the four grasping-relevant DOFs (GR-DOFs) that are affected by positions and orientations of the objects to be grasped. These four GR-DOFs include the swivel angle that measures the elbow rotation about the shoulder–wrist axis, and three wrist joint angles. For each GR-DOF, we quantify position vs orientation task-relevance bias that measures how much the DOF is affected by the grasping position vs orientation. The swivel angle and forearm supination have similar bias, and the analysis of their motion suggests two hypotheses regarding the synergistic coordination of the macro- and micro-structures of the human

arm (1) DOFs with similar task-relevance are synergistically coordinated; and (2) such synergy breaks when a task-relevant DOF is close to its joint limit without necessarily reaching the limit. This study provides a motion analysis method to reduce the control complexity for reach-to-grasp tasks, and suggests using dynamic coupling to coordinate the hand and arm of upper-limb exoskeletons.

**Keywords** Arm motion control · Task-relevance · Upper limb exoskeleton · Human-like robot

## Introduction

Wearable robots (e.g., upper-limb exoskeletons for stroke rehabilitation) must render natural arm postures kinematically compatible with their human operators. Rendering such postures is also preferred for humanoid robots, since human-like motions are more predictable and acceptable to a human partner and, therefore, facilitate smooth and comfortable human–robot interactions (Glasauer et al. 2010; Kupferberg et al. 2011). Previous research has studied how to render natural arm postures for reaching motions (Sciacchio 1987, 1988; Asada and Granito 1985; Yoshikawa 1985, 1990; Kim et al. 2011; Soechting et al. 1995; Kang et al. 2005; Hogan 1984; Flash and Hogan 1985; Uno and Suzuki 1989; Nakano et al. 1999; Milutinovic and Rosen 2014). In this paper, we further investigate posture differences between reaching and reach-to-grasp motions, to reveal the underlying arm control strategy when grasping is involved.

Human arm has kinematic redundancy which allows different arm postures given a specific hand position and orientation. This kinematic redundancy enables the rotation of the elbow position around the axis connecting the centers

✉ Zhi Li  
zli11@wpi.edu  
Dejan Milutinović  
dejan@soe.ucsc.edu  
Jacob Rosen  
jacobrosen@ucla.edu

<sup>1</sup> Department of Mechanical Engineering, Worcester Polytechnic Institute, Worcester, MA 01609, USA

<sup>2</sup> Department of Computer Engineering, University of California, Santa Cruz, Santa Cruz, CA 95064, USA

<sup>3</sup> Department of Mechanical and Aerospace Engineering, University of California, Los Angeles, Los Angeles, CA 90095, USA

of the shoulder and the wrist joints, such that the motions of reaching to grasp an object have very different arm postures compared to the reaching motions that simply transport the hand to the same position. When reaching to grasp an object, arm postures are affected by both the grasping position and orientation, not only at the moment of grasp, but also as the hand approaches the object. The motor control strategies that have successfully explained the arm postures in reaching motions cannot explain or predict such posture differences. For instance, Donders' law (Haustein 1989), which is valid for reaching motions, is not obeyed by reach-to-grasp arm motions (Tillery et al. 1995; Soechting and Flanders 1993). The jerk minimization strategy, which can render the hand paths of reach-to-grasp motions, cannot address the arm posture differences between reaching and reach-to-grasp motions (Smeets and Brenner 1999).

Previous works have studied how grasping orientation causes reach-to-grasp motions to deviate from pure reaching motions. When approaching a target, the arm movement directs the thumb to match the hand orientation with the target to grasp (Haggard and Wing 2001; Smeets and Brenner 1999). The rotation of the arm plane (formed by the positions of the shoulder, elbow and wrist) about the shoulder–wrist axis is coordinated with the supination of the forearm, to achieve the desired hand orientation. If the target orientation is perturbed when the hand is still approaching to the target, the hand path will remain approximately the same, while the hand orientation will be gradually turned from the one that matches the original target orientation to the one that matches the new target orientation (Fan and Tillery 2006). The smooth adaption to the perturbed target orientation, while maintaining the hand path, implies that a reach-to-grasp motion may be a superposition of the transportation (reaching) and manipulation (grasping) components, in which case the arm posture of a reach-to-grasp motion can be constructed by adding a grasping component to the arm posture of a pure reaching motion.

In this paper, we focus on the arm posture difference between matched reaching and reach-to-grasp motions, which cannot be addressed by the methods that can accurately predict arm postures in pure reaching motions (Sciavicco 1987, 1988; Asada and Granito 1985; Yoshikawa 1985, 1990; Kim et al. 2011; Soechting et al. 1995; Kang et al. 2005; Hogan 1984; Flash and Hogan 1985; Uno and Suzuki 1989; Nakano et al. 1999). We collected arm motion data in a three-dimensional (3D) workspace from nine participants. In a typical motion trial, a participant started with pointing at a common start position and ended with either pointing to a target or grasping the handle attached to the target in a specific orientation. We found that the hand paths of matched reaching and reach-to-grasp motions were highly similar, which indicates that not all the

DOFs of the human arm are affected by grasping an object. In the arm motion analysis, we used an arm model which can directly measure the rotation of the arm plane (i.e., the swivel angle), to identify the DOFs that behave differently in matched reaching and reach-to-grasp motions. We found that among the seven DOFs of the human arm, the swivel angle and three wrist angles contributed significantly to the arm posture differences. We, thus, consider them as highly grasping-relevant degrees of freedom (GR-DOFs) and focus on their coordination in reach-to-grasp motions.

Our study on the coordination of the GR-DOFs intends to reveal the general strategy that human arm regulates its kinematic redundancy, and to inspire the control of arm-compatible/arm-like robotic manipulators. Generally speaking, controlling a (highly) redundant robotic system is challenging because the computational cost increases exponentially with the dimension of the problem. One way to overcome the curse of dimensionality, is to distinguish redundant inputs by their task-relevance, and emphasize the regulation of the task-relevant ones while leaving the task-irrelevant ones uncontrolled. In a sit-to-stand task, human motor system could distinguish controlled from the uncontrolled manifolds, and impose more control effort on the center of mass in the sagittal plane than on the horizontal head position and the position of the hand (Scholz and Schoner 1999). For the context of a (robotic) system, the variances of a system's output are different in response to the same amount of perturbations to the system inputs in the task-relevant and -irrelevant directions (Todorov and Jordan 2002; Todorov 2004). Given the redundancy in control variables, the human motor system prefers to minimize intervention, by allowing a tolerable level of the variability of task-irrelevant variables and tightly controlling the task-relevant variables. Other research suggested that synergistic coordination of DOFs is a preferred method of control given the redundancy in the human motor system (Latash 2008). If the elements of a system are synergistically coordinated, the overall performance of the system will be stable, and will be higher than if all of elements work independently. In a synergistic coordination, the DOFs are coupled and, thus, act almost as a single unit (Turvey 2007; Santello et al. 2013). For instance, the synergistic coupling of the major finger joints, reflected by their high correlations, reduces the control complexity (Santello et al. 1998; Mason et al. 2001; Ingram et al. 2008). Studies on the arm joint coordination found that for arm motions in free space, the swivel angle deviates more from its posture in pure reaching motions as the wrist angles approach their joint limits. However, the weighting coefficients from the regression of the swivel angle with respect to the wrist angles varied largely across participants, and cannot address the arm postures' changes in structured arm motions with more rigid task constraints (Kim 2014).

In our arm motion analysis, we found that redundant DOFs were synergistically coordinated by their similarity in task-relevance. A method for quantifying the task-relevance was first proposed in our previous work (Li et al. 2014), for measuring the task-relevance of the arm joints. In other research, the task-relevance of input variables was quantified and compared using their variances (Todorov and Jordan 2002; Todorov 2004; Latash 2008). Such comparison ignores that input variables can differ in ranges and/or units, and their variances cannot be compared directly. Therefore, we propose to normalize the variance of a variable with respect to its value range (referred as the ratio of active motion range, i.e., R-AMR value). For reach-to-grasp motions, the R-ARM values of the four GR-DOFs indicate their task-relevance bias, which means if they are more sensitive to changes in grasping position or orientation. Our statistical analysis shows that among the GR-DOFs, the radial deviation is most sensitive to changes in target position, while forearm supination is most affected by target orientation. The swivel angle and forearm supination are both strongly biased towards grasping orientation in task-relevance and, therefore, are synergistically coordinated. Their synergy breaks when the forearm supination approaches its joint limit, for which their coupling should be modeled differently when they are in and out of synergy.

## Experiment

We collected data of pure reaching and reach-to-grasp motions in a three-dimensional workspace from nine participants (three males and six females, six right-handed and three left-handed, of average age  $22.9 \pm 3.2$ ). During the experiment, the participants sat in a chair with a straight back. The chair was placed so that the participant could comfortably point to each target with the elbow naturally flexed. As shown in Fig. 1a, the workspace was adjusted so that the center of the workspace was always aligned with the participant's right shoulder. The participant's right arm was free to move, while the participant's body was set against the chair back to minimize shoulder displacement. Passive reflective markers were attached to the torso and right arm of the participant, as shown in Fig. 1b. A Vicon motion capture system recorded the participant's motions at the rate of 100 Hz. Each motion trial was recorded individually, from 5–10 ms before the experimenter verbally gave a "start" command to the participant, to 20–30 ms after the subject's hand stabilized in pointing to or grasping the target.

The participants were instructed to use their right arms to conduct four sessions of reach-to-grasp motions and one session of reaching motions. Each session consisted of the motions from the common start point to eight different

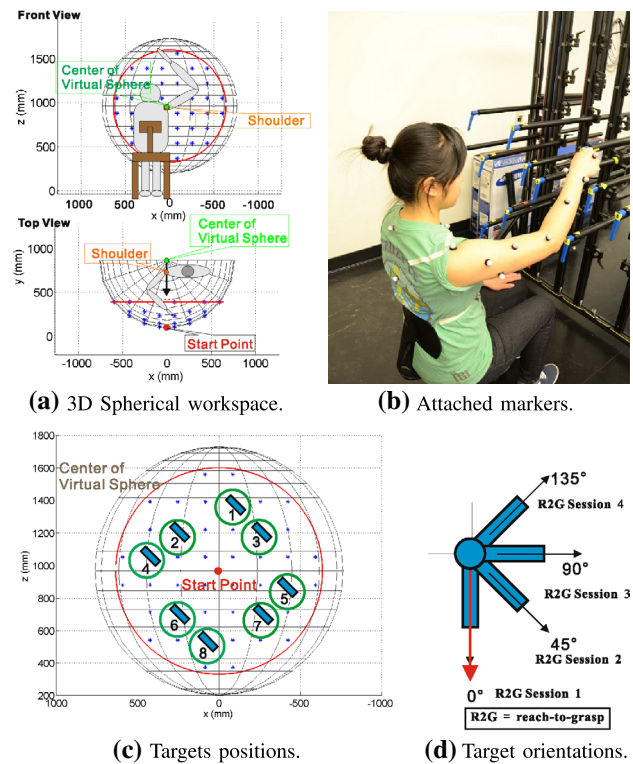


**Fig. 1** Experimental setup: **a** the right shoulder of the participant is aligned with the center of the spherical workspace; **b** markers are attached to the right arm and the torso for position tracking; **c** eight targets are involved in the reach-to-grasp experiment; **d** in the four reach-to-grasp sessions, the handles are oriented at 0°, 45°, 90°, 135° in the plane faced by the participant, with respect to the direction of gravity

targets (arranged as shown in Fig. 1c), with five repetitions. In total, each participant completed  $5 \times 8 \times 5 = 200$  trials. The participants were asked to perform all the motions at the speed of daily life activities and at a comfortable pace. In reaching trials, the participants pointed from the start point to the instructed target, with their index fingers in line with their forearms. In reach-to-grasp trials, the participants started by pointing to the start point and then reached to grasp the handle at the instructed target with a firm power grasp. The target handles were at orientations of 0°, 45°, 90°, and 135° with respect to the direction of gravity in the four reach-to-grasp sessions, respectively (see Fig. 1d). The hands of the participants traversed no more than 1.5 m in our experiments. A typical reaching/reach-to-grasp motion took 0.6–1.2 s. The time interval between two subsequent trials was about 20–30 s. Typically, it took a subject 1–2 h to complete the experiment. To avoid fatigue, the participants rested after each session and at their requests, during which their arms could rest on the chair arms. All our participants completed the five sessions within 2 h, including time for resting.

Note that in both reaching and reach-to-grasp motions, unnecessary wrist motions were intentionally reduced by natural wrist muscle tension resulting from the hand gestures that our experiment protocol required. In reaching sessions, participants were asked to point to the targets with their index fingers extended and their other fingers flexed into a fist, which naturally resulted in wrist muscle tension and, thus, kept the wrist straight. Similarly, in the reach-to-grasp sessions, a participant started with the same pointing gesture and then grasped the target handle with a firm power grasp, both of which also prevented the subject’s wrist from being floppy. Since unnecessary wrist motions were minimized, the wrist angle differences between matched reaching and reach-to-grasp motions could mostly be attributed to (1) the natural opening and closing of the hand when grasping a handle, and (2) matching the hand orientation to the target handle orientation.

### Motion analysis methodology

#### Kinematic modeling of the human arm

Traditionally, the analysis of joint coordination in reach-to-grasp motions uses a kinematic model, which is based on the anatomical joints of the human arm. As shown in Fig. 2a, the seven DOFs are: shoulder abduction  $\theta_1$ , shoulder flexion  $\theta_2$ , shoulder rotation  $\theta_3$ , elbow flexion  $\theta_4$ , forearm supination  $\theta_5$ , wrist flexion  $\theta_6$  and radial deviation  $\theta_7$ .

The swivel angle model (see Fig. 2b) we use in our motion analysis also has seven DOFs: three for the wrist position, three for the wrist orientation, and one for the swivel angle. The swivel angle measures the rotation of the elbow position about the shoulder–wrist axis, given a fixed hand position and orientation [for the details of the algorithm to compute the swivel angle, see Li et al. (2014)].

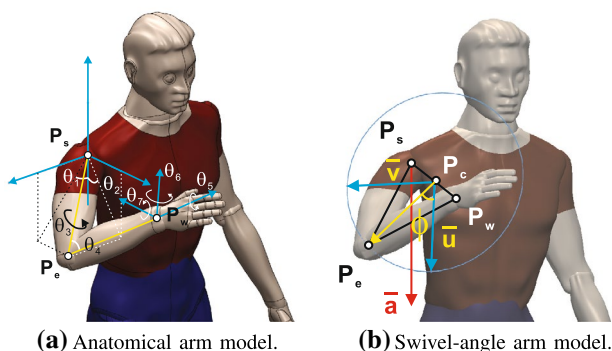


Fig. 2 Two kinematic models for the arm motion analysis [(rendered from Li et al. (2014)]

Using the swivel-angle arm model, grasping a target handle instead of pointing to it affects the four DOFs (i.e., three wrist joints and the swivel angle) that are relevant to the control of arm postures, but not the three DOFs that account for the hand position.

Using the swivel angle can simplify the motion analysis and control. In swivel-angle arm model, the changes in arm posture only affect one DOF (i.e., the swivel angle), while in the anatomical arm model, the change of arm posture will affect all the seven DOFs. Note that the swivel-angle arm model is for motion analysis but not what the human motor system uses for motion control. It can be used to analyze general arm motions in 3D workspace, including, but not limited to, reach-to-grasp and reaching motions.

Compared to a matching reaching motion, a reach-to-grasp motion has a similar hand path, but significantly different arm posture. As shown in Fig. 3, the swivel-angle arm model distinguishes the three DOFs affected by hand position from the four GR-DOFs. In the following sections, we will use the swivel-angle arm model to reduce the complexity of motion control analyses, and focus on the four GR-DOFs, i.e., the swivel angle and the three wrist joint angles.

#### Data normalization and component separation

We computed the trajectories of the seven arm joints from the recorded marker trajectories. For the four GR-DOFs, the trajectories were normalized relative to the percentage of the path length traversed by the hand (instead of time) and averaged based on five repetitions of the same motion. We computed the grasping-related differences between matched reaching and reach-to-grasp motions, and referred to them as the grasping components of the reach-to-grasp motions. The reaching and grasping components were separated for four GR-DOFs: the swivel angle and the three wrist angles.

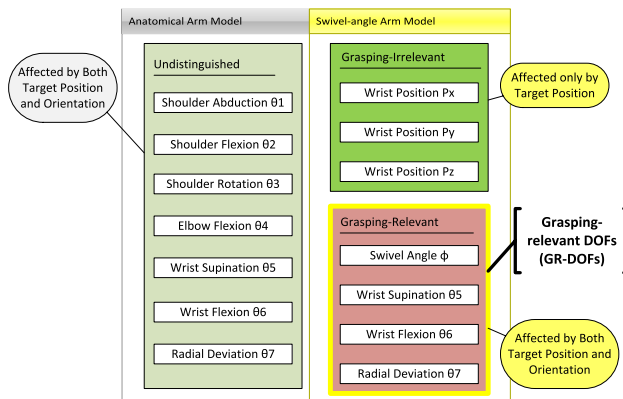
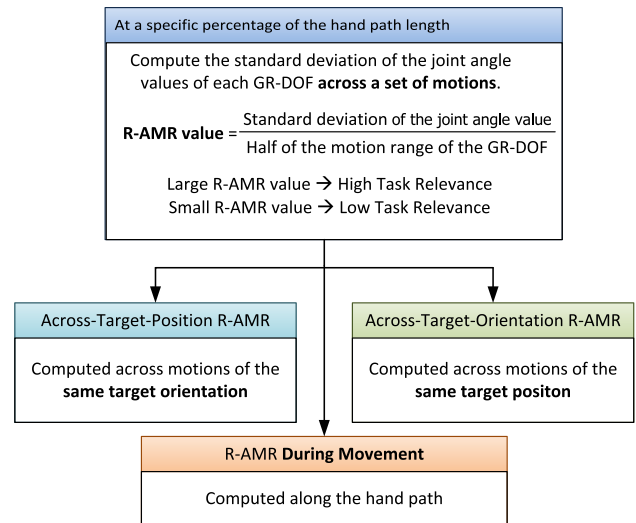


Fig. 3 Comparison between the two kinematic arm models

Figure 4 shows an example of the data normalization of the swivel angle in the trials collected from a representative participant. In Fig. 4a, swivel angle trajectories to a single target are normalized with respect to hand path length. The averaged trajectory of five repetitions of each motion is shown in Fig. 4b. With reference to the reaching motion, each reach-to-grasp motion to the same target is separated into a reaching component (Fig. 4c) and a grasping component (Fig. 4d), which is computed as the difference between the reaching motion and the reach-to-grasp motion to the same target in a specific orientation.

**Quantification of task-relevance**

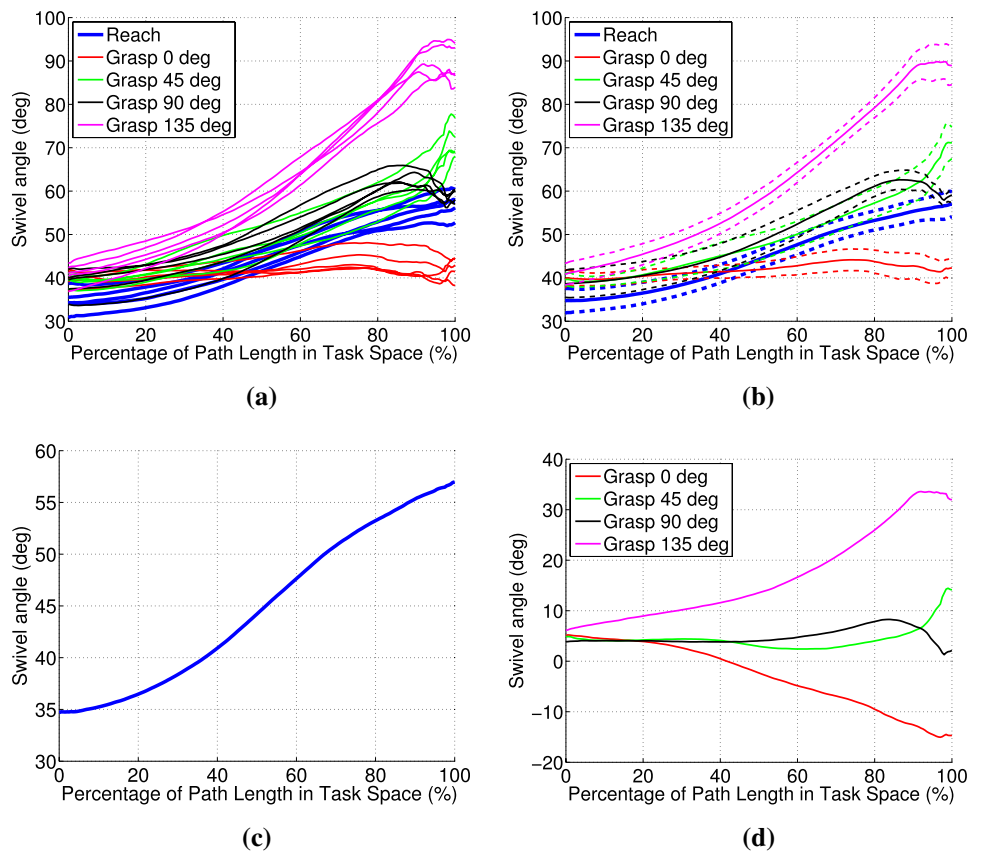
The ratio of the active motion range (R-AMR) was proposed to quantify the task-relevance of each GR-DOF (Li et al. 2014). At a specific percentage of the hand path length, we computed the standard deviation of the value of each GR-DOF across a set of motions. The R-AMR at this percentage of the hand path is the ratio between this standard deviation and a half of the motion range of the GR-DOF. As shown in Fig. 5, the R-AMR can be computed across different motion sets, including motions to targets at a particular position or in a particular orientation. For a motion set, a large R-AMR value indicates that that particular DOF is sensitive to the task parameters that vary within



**Fig. 5** R-AMR values are computed over a set of motions as the ratio between the standard deviation of the joint angles and half of the joint’s motion range, to measure task-relevance

that motion set. For example, the R-AMR of a DOF across reach-to-grasp motions towards a particular target position with different orientations indicates the sensitivity of that DOF to target orientation. Likewise, the R-AMR of a DOF across motions to different targets that share the same

**Fig. 4** A representative example of the data normalization [rendered from Li et al. (2014)]. **a** The swivel angle trajectories are normalized with respect to the percentage of path length. **b** The averaged trajectories are shown with their time-varying standard deviation. With reference to the averaged trajectory of the reaching motion, the reach-to-grasp motions can be separated into **c** the reaching component and **d** the grasping component



orientation indicates the sensitivity to target position. These across-target-orientation and across-target-position R-AMR values were computed and multiple comparisons were applied to analyze the task-relevance of each GR-DOF.

Figure 6 illustrates the computation of R-AMR values with two examples. In Example 1 of Fig. 6, we compute R-AMR values for the reaching component at swivel angle  $\phi$  at different stages of the motion, measured by the percentage of hand path length. We consider a set of motions ( $S_m$ ) from a single participant, defined as:

$$S_m = \{m(\text{targ, type}) | \text{targ} = 1 \dots 8, \text{ort} = N/A, \text{type} = R, G, R2G\}. \tag{1}$$

In Expression (1), “targ” refers to target position (chosen from 1 to 8); “type” refers to the motion (component) type and has the options of “R” for pure reaching motions (which are also reaching components), “G” for grasping components, and “R2G” for reach-to-grasp motions. For all reaching motions, the grasping orientation parameter is not available (N/A). Given the set of motions, we first compute the standard deviation of the swivel angle values in reaching motions at 20% of the path length, denoted by  $\phi_{20\%,m(\text{targ,type})}$ , for each motion  $m(\text{targ,type}) \in S_m$ . With this standard deviation, denoted by  $\sigma_{\phi_{20\%},S_m}$ , we compute the R-AMR value at 20% of the motion for this motion set, denoted by R-AMR<sub>20%</sub> as:

$$\text{R-AMR}_{20\%} = \frac{\sigma_{\phi_{20\%},S_m}}{\frac{1}{2}R_\phi}, \tag{2}$$

where  $R_\phi$  is the motion range of swivel angle. The R-AMR values for other percentages (i.e., 60, 100%) can be computed similarly.

In Example 2 of Fig. 6, we compute the R-AMR<sub>100%</sub> of the grasping components of swivel angle, for motions with different grasping orientations. When computing

R-AMR<sub>100%</sub> for grasping at 135°, we consider the set of motions from a single participant, which is:

$$S_m = \{m(\text{targ, ort, type}) | \text{targ} = 1 \dots 8, \text{ort} = 135^\circ; \text{type} = G\}. \tag{3}$$

In Eq. (3), “ort” refers to target orientation, which can be 0°, 45°, 90°, and 135°. Given the set of motions, the standard deviation is computed for the swivel angle values of the grasping component at 100% of the path length, denoted by  $\phi_{100\%,m(\text{targ,ort,type})}$ , for each motion  $m(\text{targ,ort,type}) \in S_m$ . This standard deviation, denoted by  $\sigma_{\phi_{100\%},S_m}$ , is further normalized with respect to the half of the swivel angle motion range such that for this set of motions  $S_m$ ,

$$\text{R-AMR}_{100\%} = \frac{\sigma_{\phi_{100\%},S_m}}{\frac{1}{2}R_\phi}. \tag{4}$$

### The significance of task-relevance measurement

In biological systems, motor synergy is found among motor control variables coordinated towards the same goal (e.g., fingers’ contact forces in grasping). This synergy is task-dependent and can be validated if the sum of variances of the input variables is larger than the variance of the output variable (Latash 2008, 2010). For biological systems which are usually highly redundant, eliminating the control variables with no task-relevance can simplify the motion and control analysis. Previous studies on motor synergy measured and compared the task-relevance of controlled variables using their variance (Todorov 2004; Latash 2008). However, for controlled variables with largely different value ranges and/or units, it is not valid to compare their task-relevance using their variance. Therefore, our proposed method normalizes the task-relevance measurement, so that task-relevance can be compared regardless of the variables’ value ranges and units.

For a task with multiple goals, comparing a variable’s task-relevance to different goals can identify its bias in task-relevance. For instance, the task of supporting an object with two hands has only one goal, so that the two controlled variables, i.e., the supporting forces from two arms, do not have bias in task-relevance. On the other hand, the task of reaching to grasp an object has two goals, i.e., matching the hand orientation and position to those of the target. By computing the task-relevance to each goal, we can identify the joints whose angles vary more with target orientation(position). These joints are considered to be biased in task-relevance towards target orientation (position). Joints of similar task-relevance bias are more likely to form synergistic coordination.

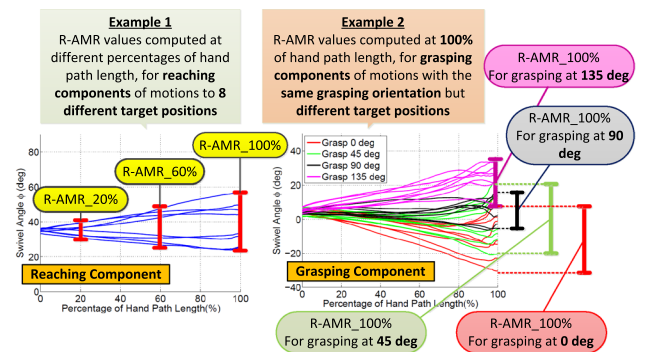


**Fig. 6** Examples: the R-AMR values computed for the reaching and grasping components, respectively. *Left* the R-AMR values during the motion are denoted by their percentages. *Right* an example of R-AMR values computed for motions to different target positions but of the same grasping orientation

## Synergy and correlation analysis

In the presence of redundant DOFs, their control complexity can be reduced by leaving the task-irrelevant DOFs uncontrolled. Furthermore, redundant DOFs can be synergistically coupled to improve overall motion performance. In the task of reaching to grasp a cylindrical object with a power grasp, human arm has two redundant DOFs. The arm kinematics has seven DOFs, while the grasping task only strictly constrains five DOFs: three for the hand position and two for grasping orientation. The arm can rotate freely about the shoulder–wrist axis (measured by the swivel angle), and the hand can rotate about the cylindrical target’s central axis (corresponding to the motion at wrist flexion). By analyzing the task-relevance of the four GR-DOFs, we found that in reach-to-grasp motion, (1) the DOFs with low task-relevance are uncontrolled and maintained close to their neutral positions with a small variance, and (2) the DOFs with high task-relevance and similar bias are synergistically coupled, which can be verified using the synergy and correlation analysis.

The synergy analysis compares the sum of the inputs’ variances and the output variance (Latash 2008). Given a system with inputs  $x_i$  ( $i = 1, \dots, n$ ) and output  $y$ , if the  $n$  inputs are in synergy, then the standard deviations of the inputs ( $\sigma_{x_i}$  for  $x_i$ ) and output ( $\sigma_y$ ) should obey:

$$\sigma_y^2 < \sum_{i=1}^n \sigma_{x_i}^2. \quad (5)$$

Synergy analysis can identify whether the coordination of input variables results in system performance improvement. On the other hand, correlation coefficient ( $r$ ) can be used to identify if several input variables are controlled in coupling (Ingram et al. 2008; Liu and Xiong 2014). A pair of joints are coupled if their joint variables have strong correlation ( $|r| \in [0.5, 1]$ ) (Cohen 1988). In this study, using both synergy and correlation analyses, we find that the swivel angle and forearm supination are synergistically coupled. We propose to apply a similar method to control the arm–hand coordination of arm-compatible robots (e.g. upper-limb exoskeletons for stroke rehabilitations), as well as the coordination of macro- and micro-structures of arm-like manipulators.

## Results

This section presents results from the motion analysis of the arm posture difference between pure reaching and reach-to-grasp motions. Prior to computing the R-AMR values for each GR-DOF as explained above, the data

collected on reach-to-grasp motions were normalized and separated into reaching and grasping components. The correlation between matched reaching and reach-to-grasp motions at each DOF demonstrates their similarity in hand path and the low grasping-relevance of the three DOFs for wrist positions. As a result, we focus on the four GR-DOFs, which are responsible for the arm posture difference. Component separation is applied to the reach-to-grasp motions at each GR-DOF [for details, refer to Li et al. (2014)]. We further computed the R-AMR values for reaching and grasping components to compare the task-relevance of different GR-DOFs during the motion and particularly at the end of the motion. Among the four GR-DOFs, the swivel angle and forearm supination collaboratively adjust the hand to match the target handle orientation that changes on the plane that the participants are facing to. Given their similar task-relevance, we further analyze their synergy and investigate their coordination for controlling the corresponding joints of an upper-limb exoskeleton.

### Hand path similarity between reaching and reach-to-grasp motions

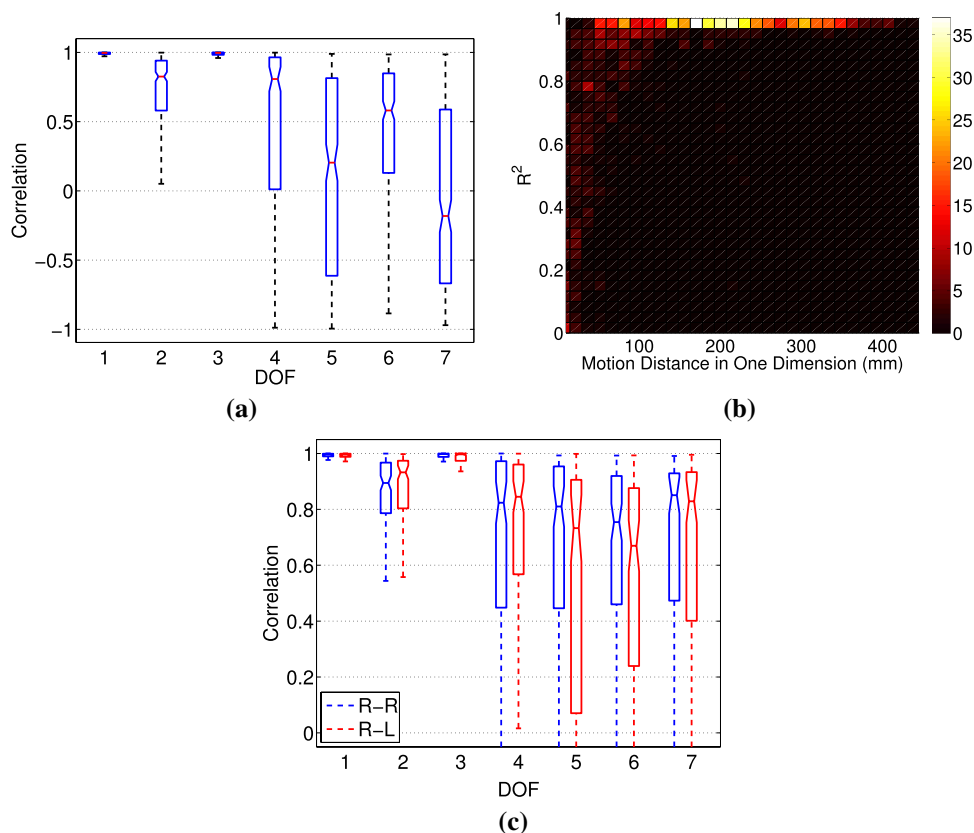
Here, we compare the corresponding reaching and reach-to-grasp motions to show their similarity in hand path. We first compute correlations of each reach-to-grasp motion to its paired reaching motion, and then compare the statistics among the seven DOFs in the swivel-angle arm model. In Fig. 7a, DOFs 1–3 correspond to the wrist position ( $P_X$ ,  $P_Y$ ,  $P_Z$ ). DOF 4 refers to the swivel angle. DOFs 5–7 are the three wrist angles  $\theta_5$ ,  $\theta_6$ , and  $\theta_7$ , respectively. Among DOFs 1–3, the correlations are close to 1 with very small variations in the X and Z dimensions (i.e., DOF 1 and 3, respectively), while in the Y-dimension (DOF 2), the correlation is relatively low, but still much higher than in the four GR-DOFs (DOFs 4–7). This similarity in hand path is consistent among the participants. As presented in Table 1, the four-way ANOVA analysis found significant differences between matched reaching and reach-to-grasping motions for the factors of target position, motion session (pointing to or grasping a target posed in different orientations), and DOFs in the arm models, but not among the participants.

In Figs. 8 and 9, we depict motions of a participant with their starting point and target handles. In the X, Y, and Z dimensions, we plotted each reach-to-grasp motion

**Table 1** Four-way ANOVA analysis compared matched reaching and reach-to-grasp motions. Significant differences in arm configurations were found for the factor of target position, motion session, DOF in the swivel arm model, but not among the participants

	Target position	Motion session	DOF	Participant
<i>p</i> value	0.0000	0.0000	0.0000	0.2454

**Fig. 7** **a** The three DOFs for wrist position (DOFs 1–3) demonstrate a high correlation between matched reaching and reach-to-grasp motions, which indicates their similarity in hand path. **b** Hand paths are more similar in a dimension if the motion distance in this dimension is large. The hand paths in Y-dimension are less similar among the three wrist DOFs, due to the wrist position differences introduced by the extended index finger pointing to the targets. **c** Comparison of motion similarity between left-handed and right-handed subjects



against its matched reaching motion, using a solid dot to indicate the beginning of a motion. As shown in Figs. 8 and 9, matched reaching and reach-to-grasp motions in the Y-dimension are highly collinear until the hand is close enough to grasp a target. As a participant started to grasp the blue handles, the wrist position increased in the positive Y direction. The Y-dimension has a larger dissimilarity in hand path than the X- and Z-dimensions. This is because at the end of a reaching trial, the participant pointed to one end of the target handle (shown as yellow dots). The extended index finger kept the wrist position further away from the target. Figure 7b further shows the effect of motion distance on the linearity of matching motion plots, measured by coefficient of determination  $R^2$ . The matched reaching and reach-to-grasp motions are highly collinear ( $R^2 > 0.85$ ) if motion distance in this dimension is more than about 10 cm. As shown in Figs. 8 and 9, compared to the motions to other targets, motions ending at Targets 1 and 8 have smaller motion distances in the X-dimension, and therefore, their matching plots in the X-dimension have worse linearity. To sum up, the relatively low correlation in Y-dimension is due to the wrist position difference introduced by the extended index finger with respect to the small motion distances in Y-dimension.

The reaching and reach-to-grasp motions requested in our experiments are neither complex nor difficult. Such

motions are widely observed in daily life and were performed by our subjects effortlessly without any training. Here, we found no significant difference among motions performed by the left-handed and right-handed subjects using their right arms. We randomly picked up three right-handed subjects and compared their motions with the motions of another three right-handed subjects, and with the three left-handed subjects. As shown in Fig. 7c, the correlation between matching motions of the R–R (right-handed V.S. right-handed) group is not significantly different from that of the R–L (right-handed V.S. left-handed) group at any DOF.

### The task-relevance during the motions

The statistical analysis of the R-AMR values during reach-to-grasp motions demonstrates that different GR-DOFs are not used to the same extent. Although human arm starts to adjust its posture to match the target orientation at an early motion stage, the wrist joint, which is responsible for the final adjustment, is not actively used until the hand is close to the target. As the use of a GR-DOF increases, the joint angle variance (due to the variance in target position and orientation) increases, reflected by the increase in its R-AMR value. To investigate the task-relevance of a GR-DOF during the motion, R-AMR values were computed

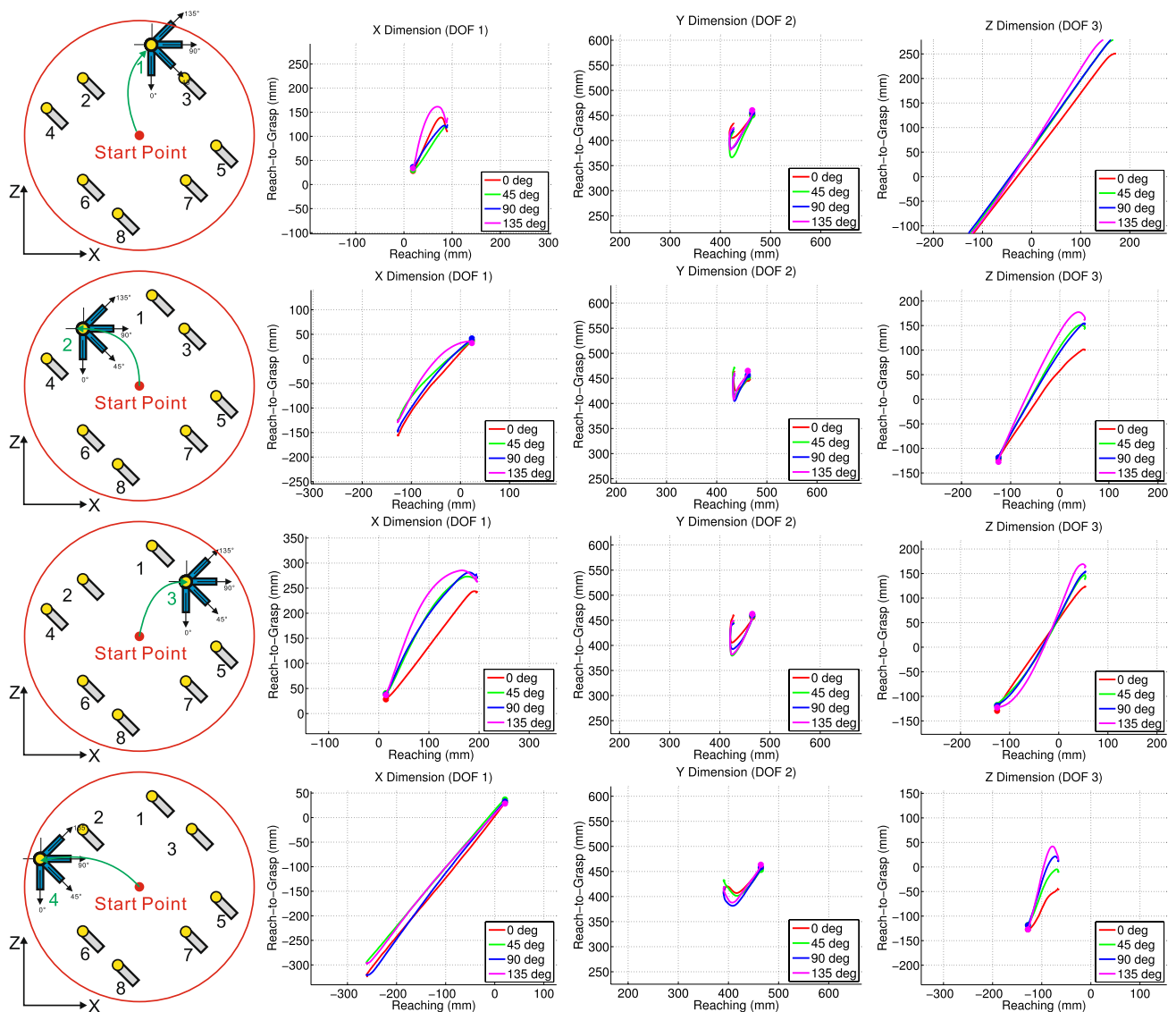


**Fig. 8** Comparison between the hand paths (represented by the 3 DOFs for wrist positions) of matched reaching and reach-to-grasp motions to Targets 1–4 from a representative participant

at each 0.5% of the hand path length. For a reaching component, R-AMR values are computed based on the standard deviations across target positions, while for a grasping component, R-AMR values are computed based on the standard deviation across target position and target orientation, respectively.

Figure 10a shows the mean R-AMR values of the reaching component during the motion. The mean R-AMR of the swivel angle quickly becomes much larger than that of the other DOFs. Figure 10 plots the mean (across participants) of the across-target-orientation R-AMR values against the mean of the across-target-position R-AMR values. Among the four profiles in Fig. 10, the slopes of the swivel angle and forearm supination are

greater than one, which implies that the swivel angle and forearm supination are more sensitive to changes in target orientation than to changes in target position. The across-target-orientation R-AMR increases roughly linearly with the across-target-position R-AMR, except for the profile for the wrist flexion. The turning in the profile for the wrist flexion is due to the natural opening and closing of the hand in preparation for grasping the target. Close to the end of the motion, the hand grasps the target handle with a firm power grasp. The muscle tension at the wrist naturally straightens the wrist flexion joint, so that in Fig. 10, the wrist flexion profile falls on the reference line that indicates equal sensitivity to both target position and orientation.

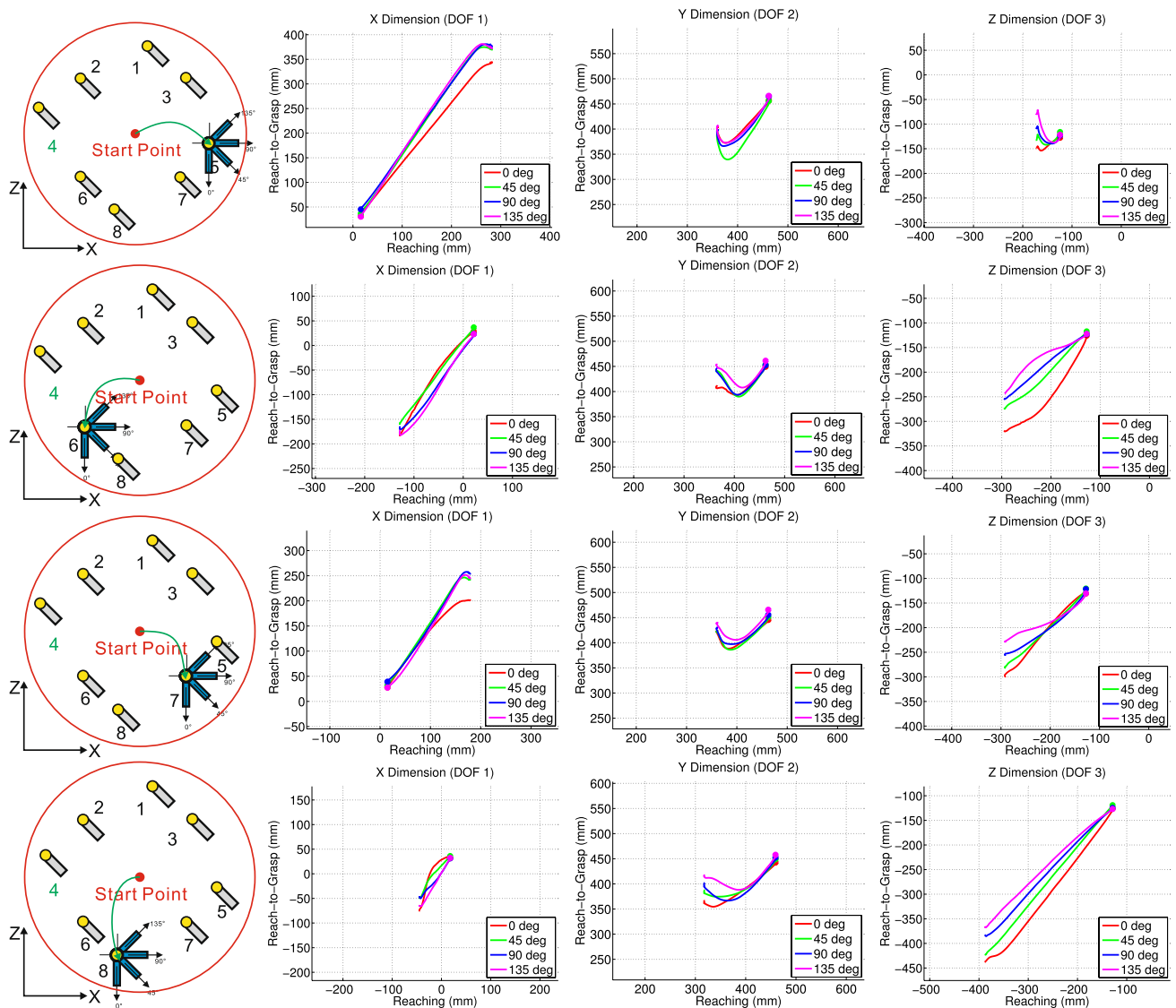
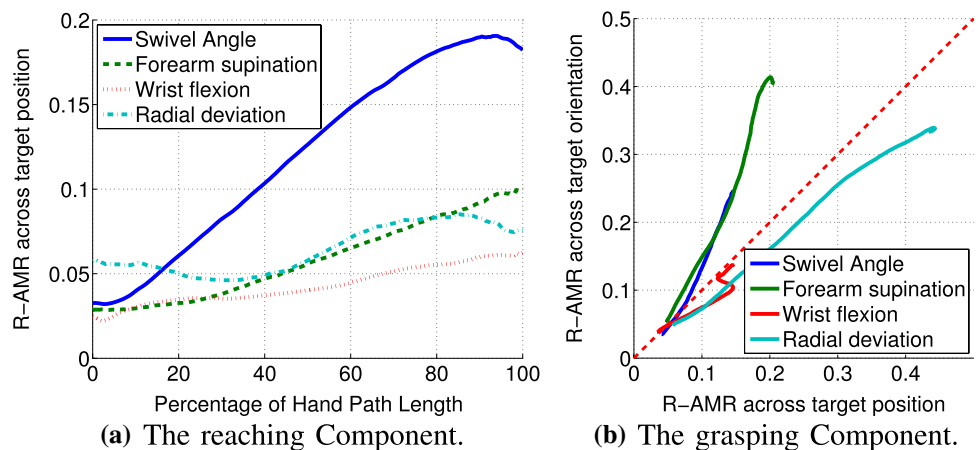


**Fig. 9** Comparison of reaching motions and reach-to-grasp motions to Targets 5–8, continued from Fig. 8

**Fig. 10** The normalized R-ARM values across target position and orientation, rendered from Li et al. (2014). **a** The mean R-AMR of the reaching component w.r.t the percentage of the path length; **b** the progression of R-AMR values of the grasping component during the motion: across-target-position vs. across-target-orientation R-AMR for each GR-DOF starting from the bottom left



**The task-relevance at the end of the motions**

The  $R-AMR_{100\%}$  value for a set of motions is the  $R-AMR$  computed at the end of the task. Figure 11 depicts  $R-AMR_{100\%}$  values for reaching and grasping components separately for each participant, and compares them using multiple comparison. For all of the GR-DOFs, the  $R-AMR_{100\%}$  of the grasping component is significantly larger than that of the reaching component. The swivel angle, which has the largest reaching-component  $R-AMR_{100\%}$ , exhibits the smallest difference between the reaching and grasping components. Among the grasping components, the forearm supination and radial deviation are much higher than the other two GR-DOFs. The wrist flexion has the lowest  $R-AMR_{100\%}$  for both the reaching and grasping components, which coincides with its limited motion due to the wrist tension in power grasps.

In Fig. 12, across-target-position and across-target-orientation  $R-AMR_{100\%}$  values are computed without component separation. In Fig. 12a, the radial deviation has significantly higher  $R-AMR_{100\%}$  across the target positions than the other GR-DOFs, which implies high task-relevance to the changes in target position. Figure 12b shows that forearm supination is the most relevant GR-DOF to the changes in target orientation, while wrist flexion is the least relevant. The swivel angle, which adjusts hand orientation by moving the whole arm, has much lower task-relevance than forearm supination.

In Fig. 13, we compare the swivel angle and the forearm supination by their end values and across-target-position grasping-component  $R-AMR_{100\%}$  values at different target orientations. Comparing Fig. 13a, b, the end values of the swivel angle increase significantly when the target orientation changes from  $90^\circ$  to  $135^\circ$ , while the changes in the forearm supination are small. Before the target orientation reaches  $90^\circ$ , the forearm supination changes more with the target orientation than the swivel angle. Comparing Fig. 13c, d, the  $R-AMR_{100\%}$  values of the swivel angle are consistently low for different target orientations, while the  $R-AMR_{100\%}$  of the forearm supination is significantly reduced as the target orientation increases and settles down when the target orientation reaches  $90^\circ$ .

**The synergetic coordination of the swivel angle and forearm supination**

During the experiment, the target orientation only changed in the plane that the participant faced (i.e., the  $X - -Z$  plane in Figs. 8, 9). The swivel angle  $\phi$  and the forearm supination  $\theta_5$  cooperatively adjusted the hand orientation about the  $Y$ -axis. The previous task-relevance analysis indicated these two DOFs were highly biased in their task-relevance towards the target orientation. When the target orientation was greater than  $90^\circ$ , the swivel angle was largely used to provide comfortable grasping postures.

**Fig. 11** Multiple comparison of the  $R-AMR$  values at the end of the motions (i.e., the  $R-AMR_{100\%}$ ) between the reaching and grasping components, rendered from Li et al. (2014). **a** The swivel angle. **b** The forearm supination. **c** The wrist flexion. **d** The radial deviation

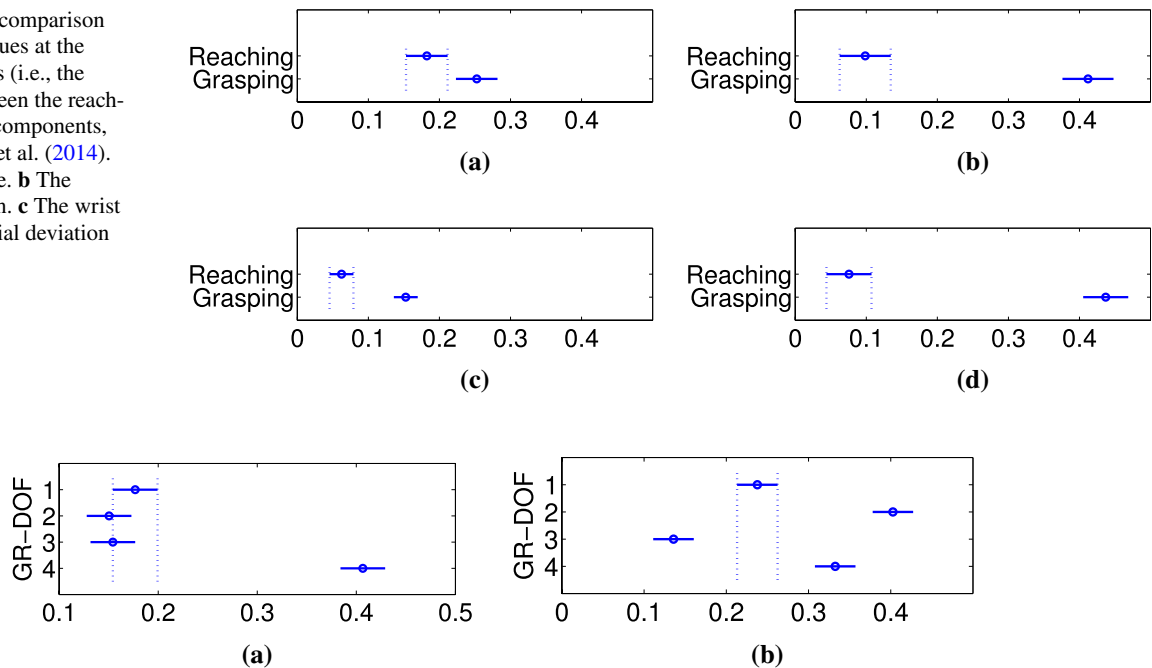
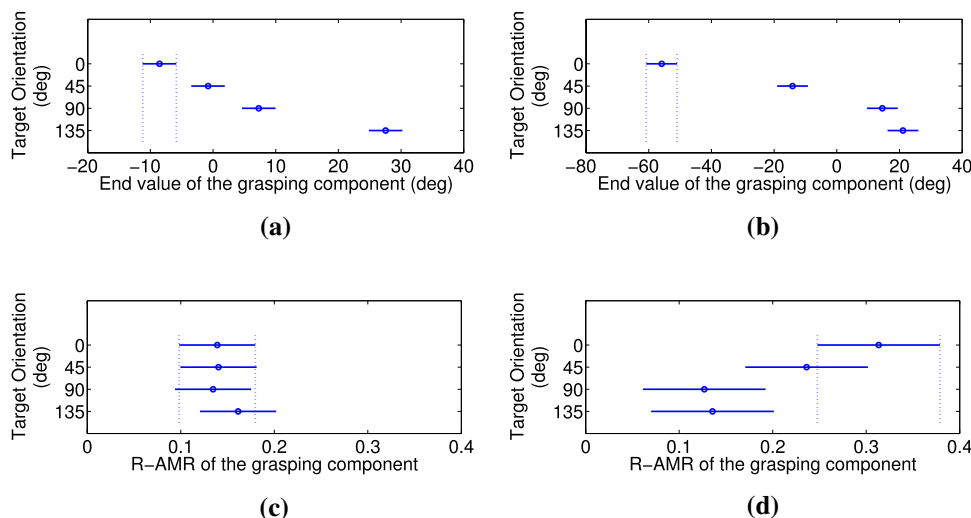


**Fig. 12** Multiple comparison of  $R-AMR_{100\%}$  values for reach-to-grasp tasks. GR-DOFs 1–4 refer to swivel angle, forearm supination, wrist flexion, and radial deviation, respectively, rendered from Li et al. (2014). **a** Across target position. **b** Across target orientation

**Fig. 13** Multiple comparison of across-target-position R-AMR<sub>100%</sub> values among different target orientations, rendered from Li et al. (2014). **a** The swivel angle. **b** The forearm supination. **c** The swivel angle. **d** The forearm supination



*Synergy and correlation analyses*

Both the swivel angle and forearm supination have high task-relevance to grasping tasks and are biased toward target orientation. We conducted synergy and correlation analyses to examine whether the swivel angle and forearm supination are synergistically coupled. For each individual reach-to-grasp motion, we computed the end value variances for (1) the swivel angle  $\phi$ , (2) the forearm supination  $\theta_5$ , and (3) the hand orientation  $\alpha$  in X–Z plane over five motion repetitions. As shown in Eq. (6), the variance difference  $\Delta_\sigma$  was computed as the difference between the sum

of the first two variances (denoted by  $\sigma_\phi$  and  $\sigma_{\theta_5}$ , respectively) and the third variance (denoted by  $\sigma_\alpha$ ):

$$\delta_{var} = \sigma_\phi^2 + \sigma_{\theta_5}^2 - \sigma_\alpha^2. \tag{6}$$

Figure 14b shows the distributions of the variance differences  $\Delta_\sigma$  for the four grasping orientations. We use a paired-samples *T* test to further compare the sum of end variances of swivel angle and forearm supination with the variance of hand orientation. According to the *p* values in Table 2, when the grasping orientation  $\alpha = 45^\circ$ , the former is significantly larger than the latter at a confidence

**Fig. 14** The distribution of variance difference  $\Delta_\sigma$  for each grasping orientation: **a** one representative participant and **b** for all participants. **c** and **d** are the results from the synergy and correlation analyses, respectively

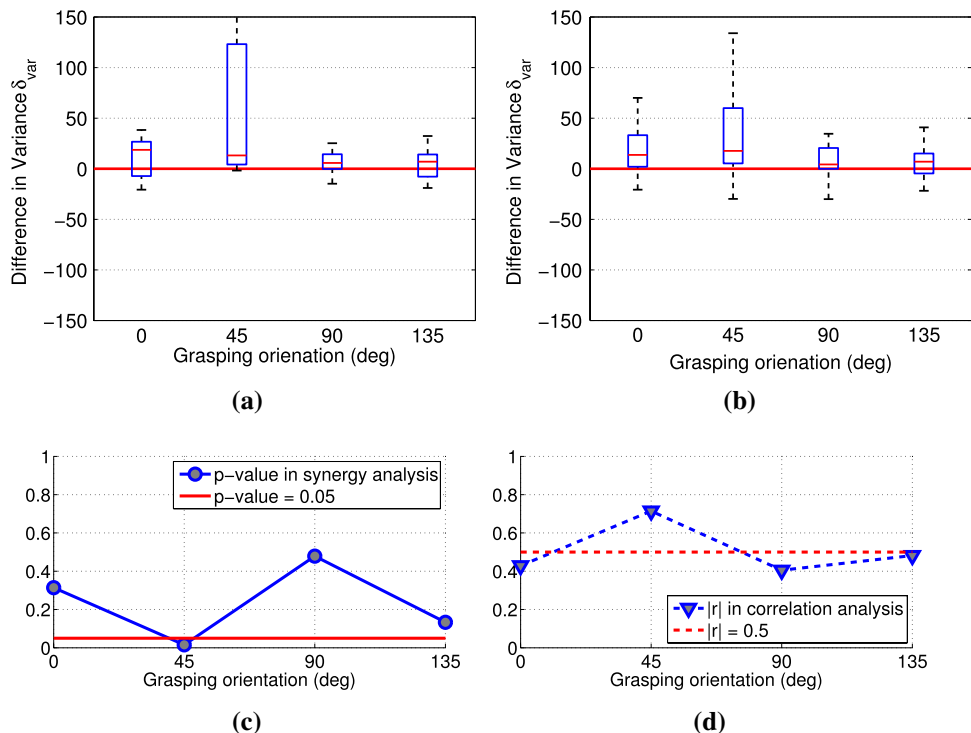


**Table 2** Results of the synergy and correlation analyses. For each grasping orientation  $\alpha$ , a significant difference exists if  $p$  value  $< 0.05$ , while the correlation is strong if  $|r| \in [0.5, 1]$

$\alpha$	0°	45°	90°	135°
$p$ value	0.3141	<b>0.0152</b>	0.4787	0.1333
$ r $	0.4285	<b>0.7143</b>	0.4052	0.4819

level of 95%, which indicates the synergistic coordination of these two GR-DOFs. We also computed the correlation coefficient for each individual motion trial instead of the averaged motion. Table 2 shows that the correlation was high for the grasping orientation of 45° ( $|r| \in [0.5, 1]$ ), and moderate for the grasping orientations of 0°, 90° and 135° ( $|r| \in [0.3, 0.5]$ ) (Cohen 1988).

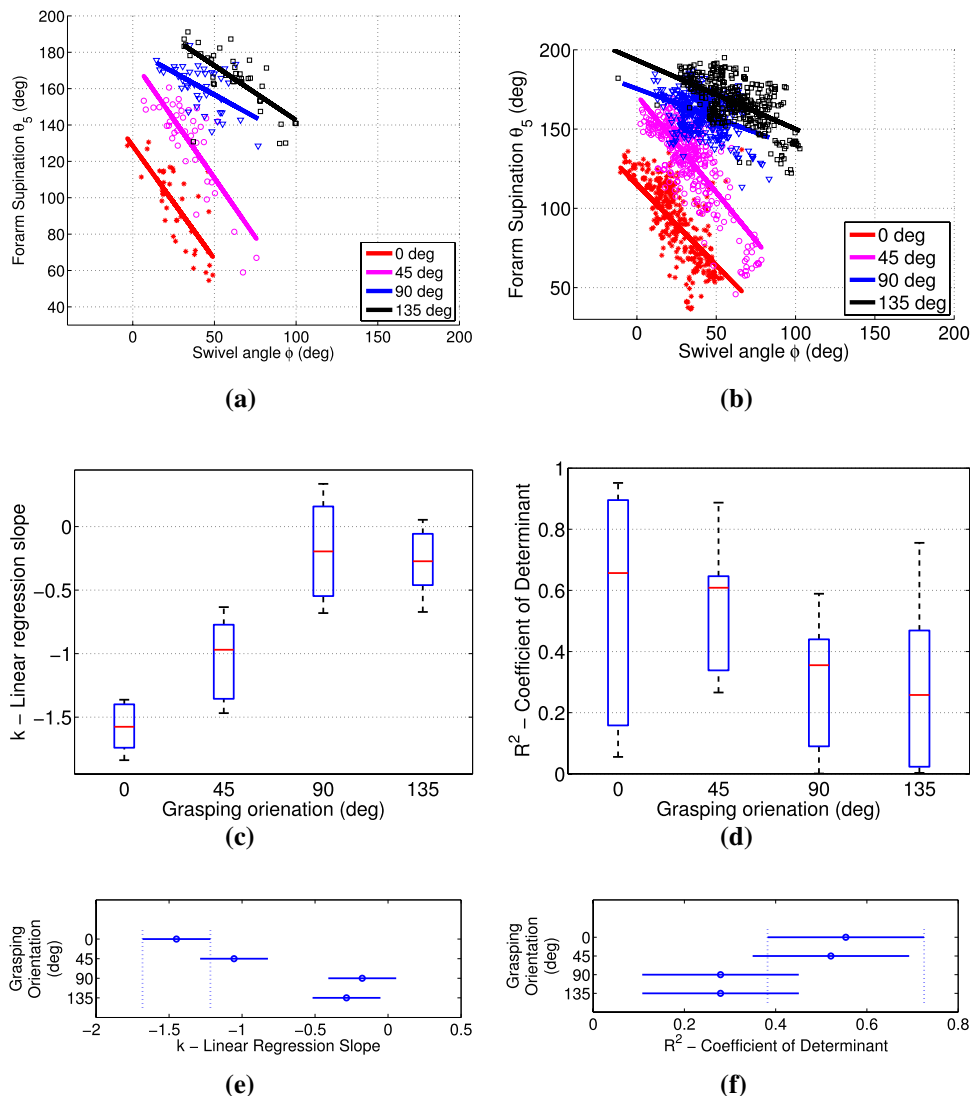
Both the synergy and correlation analyses show that the swivel angle and forearm supination are synergistically

coupled when grasping the target handles at 45° (see Fig. 14c, d). At this grasping orientation, neither of the two DOFs is close to its limits of motion ranges. When grasping the handles at 0°, the swivel angle is close to its lower limit of motion range, while grasping handles above 90°, pushes the forearm supination to its upper range limit. These results imply that the joints of high task-relevance and similar task-relevance bias are synergistically coupled. Furthermore, the synergy of coordinated joints breaks down when the joints are close to their motion range limits.

*Coupling coefficients*

In this section, we investigate the coupling coefficient between the swivel angle and forearm supination. Figure 15a shows the result of linear regression of the forearm supination over the swivel angle for a single participant, while Fig. 15 shows the result using data from

**Fig. 15** Plots of swivel angle–forearm supination pairs and their linear regressions for different grasping orientations: **a** one representative participant and **b** all participants. Distribution of linear regression parameters across participants: **c** linear regression slope  $k$ ; **d** determinant of coefficient  $R^2$  for fitting quality. **e, f** Are results of multi-comparison



all the participants. In Fig. 15c, the slope of the linear regression increases before the grasping orientation reaches 90°. For grasping orientation above 90°, the forearm supination and swivel angle maintain in small but approximately constant proportion.

The linear regression slopes indicate the ratio of joint angle change in swivel angle and forearm supination.

$$k = \frac{\theta_5(t + \delta t) - \theta_5(t)}{\phi(t + \delta t) - \phi(t)} \tag{7}$$

Equation (7) denotes the change in time as  $\delta t$ . As  $\delta t \rightarrow 0$ ,  $k$  indicates the ratio of controlled velocities. Figure 15e further shows the significant difference found by the multi-comparison of  $k$  at different grasping orientations. The joint coordinations for grasping orientations 0° and 45° are significantly different from those for the grasping orientations of 90° and 135°. Between 45° and 90°, the slope  $k$  increases faster as the forearm supination approaches its joint limit, while the linearity of the regression, measured by the coefficient of determinant  $R^2$ , dropped significantly.

The above results show that the coordination of the swivel angle and forearm supination needs to be two distinct mode. In Table 3, we summarize the mean and standard deviation of slope  $k$  with corresponding  $R^2$ . We estimate the mean value of  $k$  as a linear function of grasping orientation  $\alpha$  for grasping orientation between 0° to 90°, and as a constant for grasping orientation above 90° [see Eq. (8)].

$$k = \begin{cases} 0.0141\alpha - 1.5299 & \text{if } 0^\circ < \alpha < 90^\circ \\ -0.2307 & \text{if } 90^\circ < \alpha < 135^\circ \end{cases} \tag{8}$$

The threshold of 90° for distinct coupling modes was also suggested by our task-relevance analysis. Figure 13 has shown that above these thresholds, the swivel angle and forearm supination have very different task-relevance. The synergy and correlation analyses further show that when grasping at 45°, the swivel angle and forearm supination are in synergistic coupling. The result of this section suggests that the synergistic coordination of the swivel angle and forearm supination needs to be modeled using a varying coupling coefficient, while constant coupling coefficient can be used when their coordination is not in synergy.

**Table 3** Results of linear regression ( $\alpha$ -grasping orientation,  $k$ -linear regression slope,  $R^2$  coefficient of determination)

$\alpha$	0°	45°	90°	135°
$k$	$-1.45 \pm 0.46$	$-1.05 \pm 0.31$	$-0.18 \pm 0.38$	$-0.28 \pm 0.27$
$R^2$	$0.55 \pm 0.35$	$0.52 \pm 0.21$	$0.28 \pm 0.21$	$0.30 \pm 0.27$

## Discussion

### Comparing GR-DOFs by their task-relevance

In reach-to-grasp motions, arm posture is significantly affected by the grasp orientation. Given the similarity in matched reaching and reach-to-grasp motions, we focus on the four grasping-related DOFs that account for the differences in arm posture. To determine the control effort needed at different GR-DOFs, we compute the ratio of active motion range (R-AMR) values to measure their task-relevance. When grasping targets of different position and orientations, forearm supination and swivel angle are more sensitive to target orientation than to target position, while the other GR-DOFs are more task-relevant to target position.

In Kim (2014), the swivel angle deviation was found to be affected by the displacements of the wrist joints from their neutral positions. However, it is not clear why the forearm supination has a stronger effect on the swivel angle than the other two wrist joints. Our analysis of task-relevance provides a possible explanation to this observation: the swivel angle and forearm supination both have task-relevance to grasping task. They also have similar task-relevance bias (towards the grasping orientation in our grasping task) and, therefore, are coordinated more closely. Comparison between the grasping components of the swivel angle and the forearm supination further shows that, the forearm supination is more task-relevant than the swivel angle when the target orientations are under 90°. This is because the swivel angle adjusts the hand orientation by moving the whole arm, which consumes more energy. Before reaching the forearm supination’s joint limit, it is more energy-efficient to adjust the hand orientation by changing forearm supination.

The task-relevance analysis of the GR-DOFs of the human arm should inform the algorithms for controlling arm-compatible and arm-like robots. Control effort should be distributed based on task-relevance. Given the system redundancy, task-relevant elements should be regulated with more control effort, while task-irrelevant elements can be loosely monitored or even left uncontrolled (Todorov 2004). In our experiment, the target orientation varied in the plane that the participant faced. Therefore, both the swivel angle and the forearm supination have high task-relevance and task-relevance bias toward target orientation. To reduce the control complexity, the DOFs of high task-relevance and similar task-relevance bias can be coupled. The radial deviation also has high task-relevance with bias toward grasping orientation, and it is largely used when grasping is involved and varies more when grasping higher and lower targets. The wrist flexion has low task-relevance and no task-relevance bias when the hand grasps the target.

The DOFs of low task-relevance and weak task-relevance bias can be left uncontrolled and maintained at a neutral position.

### The synergistic coordination of the macro- and micro-structures

The analysis of the R-AMR values further shows that given similar task-relevance bias, the forearm supination is used more actively than the swivel angle for matching the hand-to-target orientation. Applied to the control of arm-like robotic manipulators, the macro- and micro-structures of the robots can be assigned different control priorities. Previous research has suggested similar control strategies to coordinate the macro- and micro-structures of arm-like manipulators. In Nakamura et al. (1987), a flexible macro-structure that moves quickly over a wide range of motion is mainly responsible for the task, while a rigid micro-structure compensates for tracking errors. In the context of reach-to-grasp motions, one way to segment the macro/micro structures refers to the arm as a macro mechanism and the hand as a micro mechanism. As such, the arm can be used as a gross positioner to maximize the dexterity of the hand for accomplishing a task (Khatib 1995; Huang et al. 2010). To adjust the hand orientation, since the swivel angle (macro) and the supination angle of the forearm (micro) can serve the same purpose, it is more energy-efficient to adjust the supination angle of the forearm as opposed to the swivel angle if the target orientation is within the forearm's range of motion.

In the synergy and correlation analyses, we further found that the swivel angle and forearm supination have similar task-relevance bias and, therefore, are in synergistic coupling when they are far from their joint limits. In the human motor system, synergy is preferred since coupling redundant elements can reduce the control complexity. Moreover, synergistic coordination can exploit the variability of the coordinated components to ensure task stability. When components are in synergy, the deviation of one component variable can be compensated by adjusting the contributions of the other components (Bernstein 1967; Scholz and Schoner 1999; Davids et al. 2006). Studies on motor synergies have investigated synergistic coordination at different levels of a motor activity (neural, muscular, dynamic, kinematic, etc.), particularly in the coordination of a large number of DOFs (for review see “Zoo of motor synergies” in Latash (2010)). However, in arm and hand motion analysis, the synergistic coordination of multiple joints was modeled using a constant coupling coefficient (Yang et al. 2002; Simkins et al. 2014; Ingram et al. 2008). Control algorithms for robot manipulators also used static couplings to mimic such joint synergy (Catalano et al. 2014). In this study, we found that the synergistic coordination of the joints of the human arm and arm-like robotic

manipulators should be modeled using a varying coupling coefficient. If any of the joints in coordination approaches to its joint limit, the synergy breaks down and their coupling can be modeled using a constant factor.

### Conclusion

We studied the arm posture difference between reaching and reach-to-grasp motions to reveal the arm motion control strategy of the human motor system in reaching and grasping tasks. We found that the hand paths of matched reaching and reach-to-grasp motions were highly similar, indicating that not all the arm DOFs are relevant to grasping tasks. Using the swivel angle model instead of the traditionally used anatomical arm model, we were able to identify the four DOFs that accounted for the arm posture differences, which reduced the motion analysis and control complexity. We further proposed the quantifier to measure the task-relevance of those GR-DOFs. Our analysis showed that among the four GR-DOFs, the wrist flexion has low task-relevance to both target position and orientation and, thus, can be left uncontrolled, to reduce the control complexity. The forearm supination and swivel angle both have strong task-relevance bias, which indicates that they might be controlled in synergistic coordination. The radial deviation has high task-relevance but no strong bias; so, it is not a candidate for coupling. Our synergy and correlation analyses revealed that the swivel angle and forearm supination are in synergy when grasping targets at 45°, but not at other orientations. The coupling between these two DOFs varies as the synergy forms and breaks down in the coordination. The coupling for grasping orientations above 90° changes significantly, after the forearm supination approaches its joint limit. Where synergy does exist, the relation between the two DOFs is much more linear. Our motion analysis suggests the control strategies for arm-compatible robots, e.g. upper-limb exoskeletons for stroke rehabilitations. For power-grasping tasks, the DOFs with low task-relevance can be maintained at their neutral positions, while the high task-relevant DOFs require more control effort. When coordinating the robot hand and arm, dynamic coupling is necessary when the synergy of the swivel angle and forearm supination exists. This guideline can be generally applied to coordinating the macro- and micro-structures of arm-like robotic manipulators.

### References

- Asada H, Granito J (1985) Kinematic and static characterization of wrist joints and their optimal design. In: ICRA 1985. St. Louis, Missouri, March 1985, pp 244–250
- Bernstein N (1967) The coordination and regulation of movements. Pergamon Press, Oxford

- Catalano M, Grioli G, Farnioli E, Serio A, Piazza C, Bicchi A (2014) Adaptive synergies for the design and control of the pisa/iit soft hand. *Brain* 33(5):768–782
- Cohen J (1988) *Statistical power analysis for the behavioral sciences*, 2nd edn. Routledge
- Davids K, Bennett S, Newell KM (2006) *Movement system variability*. Human kinetics, Champaign
- Fan J, He J, Tillery S (2006) Control of hand orientation and arm movement during reach and grasp. *Exp Brain Res* 171(3):283–296
- Flash T, Hogan N (1985) The coordination of arm movements: an experimentally confirmed mathematical model. *J Neurophysiol* 5:1688–1703
- Glasauer S (2010) Interacting in time and space: investigating human–human and human–robot joint action. In: RO-MAN, Viareggio, Italy, Sept. 2010, pp 252–257
- Haggard P, Wing A (2001) On the hand transport component of prehensile movements. *Curr Biol* 29(3):282–287
- Haustein W (1989) Considerations on listing’s law and the primary position by means of a matrix description of eye position control. *Biol Cybern* 60(6):411–420
- Hogan N (1984) An organizing principle for a class of voluntary movements. *J Neurosci* 4(2):2745–2754
- Huang J, Hara M, Yabuta T (2010) Controlling a finger-arm robot to emulate the motion of the human upper limb by regulating finger manipulability. In: Motion control, Casolo F (ed) INTECH. pp 773–792
- Ingram J, Kording K, Howard I, Wolpert D (2008) The statistics of natural hand movements. *Exp Brain Res* 188(2):223–236
- Kang T, He J, Tillery SIH (2005) Determining natural arm configuration along a reaching trajectory. *Exp Brain Res* 167:352–361
- Khatib O (1995) Inertial properties in robotic manipulation: an object-level framework. *IJRR* 5:19–36
- Kim H (2014) Systematic control and application for 7 dof upper-limb exoskeleton, Ph.D. dissertation. University of California, Santa Cruz
- Kim H, Miller L, Rosen J (2011) Redundancy resolution of a human arm for controlling a seven dof wearable robotic system. In: EMBC 2011, Boston, USA, August 2011
- Kupferberg A, Glasauer S, Huber M, Rickert M, Knoll A, Brandt T (2011) Biological movement increases acceptance of humanoid robots as human partners in motor interaction. *AI Soc* 26(4):339–345
- Latash M (2008) *Synergy*, 1st edn. Oxford University Press, USA
- Latash M (2010) Motor synergies and the equilibrium-point hypothesis. *Motor Control* 14(3):294–322
- Li Z, Gray K, Roldan J, Roldan J, Milutinovic D, Rosen J (2014) The joint coordination in reach-to-grasp movements. In: IROS. Chicago, IL, Sept. 2014, pp 906–911
- Li Z, Roldan J, Milutinović D, Rosen J (2014) Task-relevance of grasping-related degrees of freedom in reach-to-grasp movements. In: Conf Proc IEEE Eng Med Biol Soc. Chicago, IL, Aug. 2014, pp 6903–6906
- Liu M, Xiong C (2014) Synergistic characteristic of human hand during grasping tasks in daily life. *Intell Robot Appl* 8917:67–76
- Mason C, Gomez J, Ebner T (2001) Hand synergies during reach-to-grasp. *J Neurophysiol* 86(6):2896–2910
- Li Z, Milutinovic D, Rosen J (2015) Spatial Map of Synthesized Criteria for the Redundancy Resolution of Human Arm Movements. *IEEE Trans Neural Syst Rehabil Eng* 23(6):1020–1030
- Nakamura Y, Hanafusa H, Yoshikawa T (1987) Task-priority based redundancy control of robot manipulators. *IJRR* 6:3–15
- Nakano E, Imamizu H, Osu R, Uno Y, Gomi H, Yoshioka T, Kawato M (1999) Quantitative examinations of internal representations for arm trajectory planning: minimum commanded torque change model. *J Neurophysiol* 81(5):2140–2155
- Santello M, Flanders M, Soechting J (1998) Postural hand synergies for tool use. *J Neurosci* 18:10105–10115
- Santello M, Baud-Bovy G, Jorntell H (2013) Neural bases of hand synergies. *Front Comput Neurosci* 7:83–90
- Scholz JP, Schoner G (1999) The uncontrolled manifold concept: identifying control variables for a functional task. *Expe Brain Res* 126(3):289–306
- Sciavicco L (1987) A dynamic solution to the inverse kinematic problem for redundant manipulators. In: ICRA, vol. 4. Raleigh, NC, USA, Mar. 1987, pp 1081–1087
- Sciavicco L (1988) A solution algorithm to the inverse kinematic problem for redundant manipulators. *IEEE Trans Robot Automat* 4(4):403–410
- Simkins M, Al-Refai A, Rosen J (2014) Upper limb joint space modeling of stroke induced synergies using isolated and voluntary arm perturbations. *IEEE Trans Neural Syst Rehabil Eng* 22(3):491–500
- Smeets J, Brenner E (1999) A new view on grasping. *Motor Control* 3:237–271
- Soechting J, Buneo C, Herrmann U, Flanders M (1995) Moving effortlessly in three dimensions: does donders’ law apply to arm movement? *J Neurosci* 15(9):6271–6280
- Soechting J, Flanders M (1993) Parallel, interdependent channels for location and orientation in sensorimotor transformations for reaching and grasping. *J Neurophysiol* 70(3):1137–1150
- Tillery S, Ebner T, Soechting J (1995) Task dependence of primate arm postures. *Exp Brain Res* 104(1):1–11
- Todorov E (2004) Optimality principles in sensorimotor control. *Nat Neurosci* 7:907–915
- Todorov E, Jordan MI (2002) Optimal feedback control as a theory of motor coordination. *Nat Neurosci* 5:1226–1235
- Turvey MT (2007) Action and perception at the level of synergies. *Hum Mov Sci* 26:657–697
- Uno Y, Kawato M, Suzuki R (1989) Formation and control of optimal trajectory in human multijoint arm movement—minimum torque-change model. *Biol Cybern* 61:89–101
- Yang N, Zhang M, Huang C, Jin D (2002) Synergic analysis of upper limb target-reaching movements. *J Biomech* 35:739–746
- Yoshikawa T (1990) *Foundations of robotics: analysis and control*. The MIT Press
- Yoshikawa T (1985) Dynamic manipulability of robot manipulators. In: IEEE International Conference on Robotics and Automation, St. Louis, Missouri, USA, March 1985, pp 1033–1038